Inorganica Chimica Acta, *161* (1989) 49–56

Spectroscopic and Electrochemical Studies of some α-Diimine Complexes of Platinum(II) and Palladium(II) with Azide and Chloride

S. S. KAMATH, V. UMA and T. S. SRIVASTAVA*

Department of Chemistry, Indian Institute of Technology, Powai, Bombay 400 076 (India)

(Received December 3, 1988)

Abstract

Six new complexes of the formula $[M(N\text{-}N)X_2]$ (where M = Pd(II) or Pt(II), N-N = 2,2′-biquinoline or 4,7-diphenyl-1,10-phenanthroline, and $X = Cl^-$ or N_3^-) have been prepared and characterized by conductivity measurements, cyclic voltammetry, ultraviolet–visible, infrared and ^{1}H NMR spectral studies. The above and other related square planar complexes show major four bands in the ultraviolet–visible absorption region and they are assigned to $d \rightarrow \pi^*$ charge-transfer and $\pi \rightarrow \pi^*$ transitions. Cyclic voltammetry studies show that these complexes undergo electron transfer reactions with charges +1, 0, −1 and −2. The low energy absorption band and one electron oxidation and reduction potential data of the above complexes can be interpreted by the molecular orbital model used earlier for *cis*-$[Pt(py)_2Cl_2]$ (where py is pyridine). Detailed ^{1}H NMR studies on the above complexes have been carried out and the peak assignments for each proton have been made.

Introduction

$[Pt(bipy)Cl_2]$ (where bipy is 2,2′-bipyridine) in chloroform solution on irradiation at 280 nm undergo photochemical oxidative addition reaction [1]. $[Pt(bipy)X_2]$ and $[Pt(phen)X_2]$ (where phen is 1,10-phenanthroline and X^- is Cl^- or N_3^-) photosensitize the production of singlet molecular oxygen on irradiation between 300 and 800 nm. However, $[Pt(bipy)(N_3)_2]$ and $[Pt(phen)(N_3)_2]$ are much better sensitizers than the corresponding chloro derivatives [2]. In view of the importance of platinum(II) and palladium(II) complexes in photochemistry, we report here the synthesis, spectroscopic and electrochemical studies of several α-diimine platinum(II) and palladium(II) complexes with azide and chloride.

Experimental

Starting Materials

Potassium tetrachloroplatinate(II) (Strem, U.S.A.), palladium chloride, 1,10-phenanthroline monohydrate (SRL, India), 2,2′-biquinoline, 4,7-diphenyl-1,10-phenanthroline (Loba, India), tetra(n-butyl)ammonium perchlorate (Fluka, Switzerland) and sodium azide (Riedel, F.R.G.) of reagent grade were bought and used as such. 2,2′-Bipyridine and sodium chloride (Merck, India) of G.R. grade were used. The reagent grade solvents were used after purification by the standard methods [3].

Synthetic Procedures

$[M(N\text{-}N)Cl_2]$ (where M is Pd(II) or Pt(II) and N-N is 2,2′-bipyridine, 1,10-phenanthroline or 2,2′-biquinoline (biq)) were prepared by the literature methods [4–6]. They were characterized by the reported procedures [7, 8]. $[M(N\text{-}N)(N_3)_2]$ (where M is Pd(II) or Pt(II) and N-N is 2,2′-bipyridine or 1,10-phenanthroline) were prepared and characterized by the literature method [9].

[Pd(dpp)Cl$_2$]

$[Pd(dpp)Cl_2]$ (where dpp is 4,7-diphenyl-1,10-phenanthroline) was prepared by dissolving 1 mmol of $PdCl_2$ and 4 mmol of sodium chloride in 250 ml of distilled water. The solution was stirred for 3 h and the solution was filtered. 4,7-Diphenyl-1,10-phenanthroline (1 mmol) dissolved in 10 ml methanol was added to the above filtrate. The mixture was stirred for 4 h to get a precipitate of the desired complex. The complex was recrystallized from dimethyl sulphoxide (DMSO) to get yellow coloured crystals. The crystals were washed and dried in a vacuum desiccator over anhydrous calcium choride.

[Pt(dpp)Cl$_2$]

The complex was prepared by dissolving 1 mmol of K_2PtCl_4 in 1 litre of double distilled water. 4,7-Diphenyl-1,10-phenanthroline (1 mmol) and sodium chloride (4 mmol) dissolved in 1:10 methanol–water mixture and concentrated hydrochloric acid (2 ml).

---

*Author to whom correspondence should be addressed.

This mixture was added to the above K_2PtCl_4 solution dropwise and was kept in an incubator for a fortnight to get the desired complex. The complex was recrystallized from DMSO. The crystals were dried in a vacuum desiccator over anhydrous calcium chloride.

[Pd(biq)(N$_3$)$_2$], [Pt(biq)(N$_3$)$_2$], [Pd(dpp)(N$_3$)$_2$] and [Pt(dpp)(N$_3$)$_2$]

These were prepared by the general method as given below.

[M(N-N)Cl_2] (1 mmol) was dissolved in 20 ml of dimethylformamide (DMF). Sodium azide (2 mmol) dissolved in 10 ml of methanol was added dropwise to the first solution. The solution was stirred for 4 h, filtered and then concentrated on a water bath at ~50 °C. Additional methanol was added dropwise to the concentrated solution and was then kept in a refrigerator overnight. The crystals obtained were filtered. The complex was recrystallized from acetone and dried in a vacuum desiccator over anhydrous calcium chloride.

The chemical analyses of the above complexes were performed at the Microanalytical Laboratory, I.I.T., Bombay and R.S.I.C., Central Drug Research Institute, Lucknow, India.

Physical Measurements

The infrared spectra of the complexes were recorded on a Nicolet 5DXB FT-IR spectrophotometer in the range 4000 to 400 cm^{-1} as KBr pellets and on a Pye-Unichem SP-2000 infrared spectrophotometer in the range 4000 to 400 cm^{-1} as Nujol mulls. The electronic absorption spectra of the complexes in different solvents were recorded in a Shimadzu UV-260 UV–Vis recording spectrophotometer. The ^1H NMR (nuclear magnetic resonance) spectra of the complexes were recorded on a Brucker AM-500 FT-NMR spectrometer in deuterated dimethyl sulphoxide (DMSO-d_6) using tetramethylsilane as internal reference in the range of 0 to 10 ppm. The conductivity measurements of the complexes in dimethylformamide (DMF) were carried out on a systronics conductivity bridge 305 using a conductivity cell having a cell constant of 0.0784 cm^{-1}. The cyclic voltammograms of the complexes in acetonitrile (3×10^{-3} M) containing 0.1 M of tetra-(n-butyl)ammonium perchlorate as supporting electrolyte were taken on a Model CV-IB Bioanalytical Cyclic Voltammetry apparatus equipped with an Omnigraphic 2000 Recorder. A single compartment cell was employed with a Ag/AgCl reference electrode (−0.35 V versus standard calomel electrode), a platinum wire counter electrode and a platinum working electrode. The scan rate usually used was 200 mV/s and the variation in scan rate was from 2 to 200 mV/s.

Results and Discussion

Six new complexes of the formulae [M(dpp)Cl_2] and [M(N-N)(N_3)$_2$] (where M = Pd(II) or Pt(II), and N-N = 2,2′-biquinoline or 4,7-diphenyl-1,10-phenanthroline) have been prepared. The molar conductance data, and chemical analyses of these complexes and other four azido complexes are given in Table 1. The molar conductance data of these complexes suggest them to be nonelectrolytes [10].

The changes in the infrared spectra in the ligand moiety of the above complexes are compared to the free ligands suggest the coordination of ligands to metal. The presence of two strong bands between 1900 to 2000 cm^{-1} in the azido complexes is due to azide stretching vibrations and this suggests the bonding of azido groups to metal [11]. In addition the $\delta(N_3)$ and $\nu(M{-}N)$ in the azide complexes are observed around 570 and 410 cm^{-1} respectively [11].

The 500 MHz ^1H NMR spectral data of the complexes in DMSO-d_6 are given in Table 2. The structure and numbering scheme of the ligand protons of the complexes are given in Fig. 1. The α-diimine ligand protons on complexation show downfield shifts in the chloro complexes [12]. When the chemical shifts of the α-diimine ligand protons of the azido complexes are compared with the corresponding chloro complexes, they experience upfield shift with the exception of 2,2′-biquinoline complexes. The upfield shift behaviour in the above complexes is due to the stronger bonding of the azide ions to the metal ion than that of the chloride ions and more back bonding from the metal to the α-diimine ligand in the azido complexes than in the chloro complexes [13, 14].

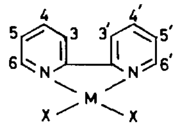

A: [M(bipy)X_2]
(M = Pd(II) and Pt(II),
X^- = Cl^- and N_3^-)

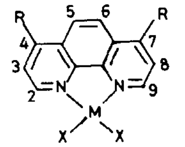

B: [M(phen) X_2] and
[M(dpp) X_2] (M = Pd(II) and
Pt(II); X^- = Cl^- and N_3^-;
R = H in phen and
R = C_6H_5 in dpp)

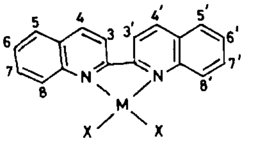

C: [M(biq) X_2]
(M = Pd(II) and Pt(II);
X^- = Cl^- and N_3^-)

Fig. 1. A to C structures and numbering scheme of [M(N-N)-X_2].

TABLE 1. Colour, yield, molar conductance and elemental analysis data of $[M(N\text{-}N)(N_3)_2]$ and $[M(dpp)Cl_2]$

Complex	Colour	Yield (%)	Molar conductance[a]	Calculated (found) (%)		
				C	H	N
$[Pd(bipy)(N_3)_2]$	yellow	50	3.40	34.64 (explosive)	2.30	32.33 (31.64)
$[Pt(bipy)(N_3)_2]$	orange–yellow	52	4.50	27.57 (28.05)	1.80 (2.10)	25.74 (24.97)
$[Pd(biq)(N_3)_2]$	black–red	64	4.90	48.39 (48.39)	2.69 (2.86)	25.09 (24.88)
$[Pt(biq)(N_3)_2]$	dark brown	60	2.60	40.38 (40.62)	2.24 (2.35)	20.92 (20.79)
$[Pd(phen)(N_3)_2]$	yellow	60	4.50	38.92 (39.00)	2.16 (2.94)	30.27 (29.76)
$[Pt(phen)(N_3)_2]$	yellow	50	4.50	31.37 (31.80)	1.74 (2.13)	24.40 (24.17)
$[Pd(dpp)(N_3)_2]$	light green	60	4.90	55.13 (54.95)	3.06 (2.86)	21.44 (20.54)
$[Pt(dpp)(N_3)_2]$	greenish–yellow	60	4.90	47.10 (47.37)	2.62 (2.54)	18.32 (18.04)
$[Pd(dpp)Cl_2]$	yellow	60	2.60	56.54 (55.18)	3.14 (3.20)	5.50 (5.24)
$[Pt(dpp)Cl_2]$	yellow	58	4.90	48.12 (47.25)	2.67 (3.88)	4.68 (4.98)

[a] Molar conductance in $cm^2\ ohm^{-1}\ mol^{-1}$.

TABLE 2. 500 MHz ^1H NMR spectral data of $[M(N\text{-}N)X_2]$ complexes in DMSO-d_6

Complex/ligand (N-N)	2,2′-Bipyridine/2,2′-biquinoline protons					
	$\delta_{H_{3,3'}}$[a]	$\delta_{H_{4,4'}}$	$\delta_{H_{5,5'}}$	$\delta_{H_{6,6'}}$	$\delta_{H_{7,7'}}$	$\delta_{H_{8,8'}}$
bipy	8.39(d)[b] $J_{3,4}$ = 8.00[c]	7.90(t)	7.40(t)	8.67(d) $J_{5,6}$ = 6.00		
$[Pd(bipy)Cl_2]$	8.59(d) $J_{3,4}$ = 7.99	8.36(t)	7.81(t)	9.12(d) $J_{5,6}$ = 5.29		
$[Pt(bipy)Cl_2]$	9.10(d) $J_{3,4}$ = 8.07	8.93(t)	8.36(t)	10.01(d) $J_{5,6}$ = 5.64		
$[Pd(bipy)(N_3)_2]$	8.55(t)	8.34(t)	7.81(t)	8.55(t)		
$[Pt(bipy)(N_3)_2]$	8.45(m)	8.45(m)	7.79(m)	8.89(d)		
biq	8.81(d) $J_{3,4}$ = 8.57	8.59(d)	8.09(d) $J_{5,6}$ = 8.11	7.69(t)	7.86(t)	8.20(d) $J_{7,8}$ = 8.44
$[Pd(biq)Cl_2]$	8.97(d) $J_{3,4}$ = 8.45	8.76(d)	8.32(d) $J_{5,6}$ = 8.61	8.03(d)	8.15(d)	8.52(d) $J_{7,8}$ = 8.61
$[Pt(biq)Cl_2]$	9.07(d) $J_{3,4}$ = 8.37	8.84(d)	8.23(t)	7.82(d)	8.02(t)	8.67(d) $J_{7,8}$ = 8.02
$[Pd(biq)(N_3)_2]$	9.02(d) $J_{3,4}$ = 8.54	8.85(d)	8.22(d) $J_{5,6}$ = 7.83	7.86(t)	8.11(t)	8.72(d) $J_{7,8}$ = 8.45
$[Pt(biq)(N_3)_2]$	9.08(d) $J_{3,4}$ = 8.34	8.81(d)	8.25(d) $J_{5,6}$ = 7.72	7.88(t)	8.02(t)	8.81(d)

(continued)

TABLE 2. *(continued)*

Complex/ligand (N-N)	1,10-Phenanthroline/4,7-diphenyl-1,10-phenanthroline protons			
	$\delta_{H_{2,9}}$ [a]	$\delta_{H_{3,8}}$	$\delta_{H_{4,7}}$	$\delta_{H_{5,6}}$
phen	9.20(d) [b] $J_{2,3} = 4.00$ [c]	7.54(q)	8.56(d) $J_{3,4} = 8.00$	8.20(s)
[Pd(phen)Cl$_2$]	9.36(d) $J_{2,3} = 4.98$	8.15(t)	8.99(d) $J_{3,4} = 8.41$	8.29(s)
[Pt(phen)Cl$_2$]	9.69(d) $J_{2,3} = 6.00$	8.15(q)	9.03(d) $J_{3,4} = 8.00$	8.28(s)
[Pd(phen)(N$_3$)$_2$]	8.94(d) $J_{2,3} = 8.22$	8.11(m)	8.80(d) $J_{3,4} = 5.03$	8.26(s)
[Pt(phen)(N$_3$)$_2$]	9.14(d) $J_{2,3} = 6.00$	8.12(m)	8.99(d) $J_{3,4} = 8.00$	8.25(s)
dpp	9.18(d) $J_{2,3} = 4.16$	7.73(d)	7.60(s) [d]	7.87(s)
[Pd(dpp)Cl$_2$]	9.41(d) $J_{2,3} = 5.17$	8.14(d)	7.69(m)	8.12(s)
[Pt(dpp)Cl$_2$]	9.68(d) $J_{2,3} = 5.56$	8.15(d)	7.72(m)	8.13(s)
[Pd(dpp)(N$_3$)$_2$]	8.92(d) $J_{2,3} = 4.90$	8.13(s)	7.68(m)	8.11(s)
[Pt(dpp)(N$_3$)$_2$]	9.28(d) $J_{2,3} = 5.36$	8.13(s)	7.53(m)	8.10(s)

[a] Chemical shifts are given in δ, ppm. [b] s, d, t, q and m are singlet, doublet, triplet, quartet and multiplet respectively. [c] *J* is coupling constant in Hz. [d] Protons of phenyl groups.

In the ^{1}H NMR spectrum of [Pd(bipy)Cl$_2$] the 2,2′-bipyridine protons $H_{6,6'}$, $H_{3,3'}$, $H_{4,4'}$ and $H_{5,5'}$ experience downfield shifts of 0.45, 0.20, 0.46 and 0.41 ppm respectively as compared to the corresponding protons of free 2,2′-bipyridine [15]. In [Pd(bipy)(N$_3$)$_2$] the 2,2′-bipyridine protons $H_{6,6'}$ and $H_{3,3'}$ show upfield shifts of 0.57 and 0.04 ppm respectively as compared to the corresponding protons in [Pd(bipy)Cl$_2$] (see Table 2). In [Pt(bipy)-Cl$_2$] $H_{6,6'}$, $H_{3,3'}$, $H_{4,4'}$ and $H_{5,5'}$ show downfield shifts of 1.34, 0.71, 1.03 and 0.96 ppm respectively as compared to the free ligand. However, $H_{6,6'}$ and $H_{3,3'}$ of [Pt(bipy)(N$_3$)$_2$] show upfield shifts of 1.12 and 0.65 ppm respectively as compared to the $H_{6,6'}$ and $H_{3,3'}$ protons of [Pt(bipy)Cl$_2$].

The $H_{3,3'}$, $H_{4,4'}$, $H_{5,5'}$, $H_{6,6'}$, $H_{7,7'}$ and $H_{8,8'}$ protons of [Pd(biq)Cl$_2$] show downfield shifts of 0.16, 0.17, 0.23, 0.34, 0.29 and 0.32 ppm respectively as compared to the corresponding protons of free 2,2′-biquinoline [15]. [Pd(biq)(N$_3$)$_2$] shows downfield shifts of 0.21 for $H_{3,3'}$, 0.26 for $H_{4,4'}$, 0.13 for $H_{5,5'}$, 0.17 for $H_{6,6'}$, 0.25 for $H_{7,7'}$ and 0.52 ppm for $H_{8,8'}$ respectively as compared to the corresponding protons of the free 2,2′-biquinoline ligand. [Pt(biq)Cl$_2$] shows downfield shifts of 0.26 for $H_{3,3'}$, 0.25 for $H_{4,4'}$, 0.14 for $H_{5,5'}$, 0.13 for $H_{6,6'}$, 0.16 for $H_{7,7'}$ and 0.47 ppm for $H_{8,8'}$ respectively as compared to the corresponding protons of free ligand. Similarly [Pt(biq)(N$_3$)$_2$] has downfield shifts of 0.27 for $H_{3,3'}$, 0.22 for $H_{4,4'}$, 0.16 for $H_{5,5'}$, 0.19 for $H_{6,6'}$, 0.16 for $H_{7,7'}$ and 0.61 ppm for $H_{8,8'}$, respectively as compared to the corresponding protons of the free ligand.

The $H_{2,9}$, $H_{4,7}$, $H_{5,6}$ and $H_{3,8}$ protons of [Pd-(phen)Cl$_2$] experience downfield shifts of 0.16, 0.43, 0.09 and 0.61 ppm respectively as compared to the corresponding protons of free 1,10-phenanthroline [15]. The $H_{2,9}$ and $H_{4,7}$ protons of [Pd(phen)(N$_3$)$_2$] show upfield shifts of 0.42 and 0.19 ppm respectively as compared to the $H_{2,9}$ and $H_{4,7}$ protons of [Pd(phen)Cl$_2$]. Similarly the $H_{2,9}$, $H_{4,7}$, $H_{5,6}$ and $H_{3,8}$ protons of [Pt(phen)Cl$_2$] experience downfield shifts of 0.49, 0.47, 0.08 and 0.61 ppm respectively as compared to the free ligand. The $H_{2,9}$ and $H_{4,7}$ protons of [Pt(phen)(N$_3$)$_2$] show upfield shifts of 0.55 and 0.04 ppm respectively as compared to the $H_{2,9}$ and $H_{4,7}$ protons of [Pt(phen)Cl$_2$].

The $H_{2,9}$, $H_{3,8}$ and $H_{5,6}$ protons of [Pd(dpp)Cl$_2$] show downfield shifts of 0.23, 0.41 and 0.25 ppm respectively as compared to the corresponding protons in free 4,7-diphenyl-1,10-phenanthroline [15]. However, the protons $H_{2,9}$ and $H_{3,8}$ of [Pd-

$(dpp)(N_3)_2]$ have upfield shifts of 0.49 and 0.01 ppm respectively as compared to the $H_{2,9}$, $H_{3,8}$ protons of $[Pd(dpp)Cl_2]$. Similarly the $H_{2,9}$, $H_{3,8}$ and $H_{5,6}$ protons of $[Pt(dpp)Cl_2]$ show downfield shifts of 0.50, 0.42 and 0.26 ppm respectively as compared to the corresponding protons of the free ligand. The $H_{2,9}$ and $H_{3,8}$ protons of $[Pt(dpp)(N_3)_2]$ show upfield shifts of 0.40 and 0.02 ppm respectively as compared to the $H_{2,9}$ and $H_{3,8}$ protons of $[Pt(dpp)Cl_2]$.

The electronic absorption spectra of the chloro and azido complexes in DMF show 4 (or 5) band maxima. The positions of these bands with extinction coefficients are given in Table 3. These bands are assigned on the basis of band assignments of chloro complexes as reported earlier [7]. The bands 1 and 3 are assigned to charge transfer transitions from metal d-orbital to π-anti-bonding orbitals of α-diimine ($d \rightarrow \pi^*$). The bands 2 and 4 are assigned to intraligand $\pi \rightarrow \pi^*$ transition of α-diimine. These band assignments are supported by the blue shift of 10–15 nm of bands 1 and 3 and shift of 0–3 nm of bands 2 and 4 from less polar to more polar solvents. The plot of Reichardt's parameter (E_T) of the solvents against absorption maxima gives two separate lines, one for hydroxylic solvents and other for non-hydroxylic solvents [7, 16, 17]. A typical plot for $[Pd(bipy)(N_3)_2]$ is given in Fig. 2.

If the molecular orbital (MO) diagram for *cis*-$[Pt(pyridine)_2Cl_2]$ in C_{2v} symmetry [18] is used for $[M(N\text{-}N)X_2]$ (C_{2v} symmetry), the HOMO (highest occupied MO) is predominately the $d_{x^2-y^2}$ orbital and LUMO (lowest unoccupied MO) is the π^* orbital of α-diimine. The transition between HOMO to LUMO leads a charge transfer transition corresponding to band 1 in $[M(N\text{-}N)X_2]$. The higher energy of band 1 in $[Pd(N\text{-}N)X_2]$ as compared to its value in corresponding $[Pt(N\text{-}N)X_2]$ (see Table 3) can be explained because the $d_{x^2-y^2}$ orbital has a higher energy in the latter complexes than in the former complexes. The higher energy band 1 in $[M(phen)X_2]$ than in corresponding $[M(dpp)X_2]$ (see Table 3) can also be explained because the LUMO energy of α-diimine is lower in dpp than in phen. This LUMO energy lowering in dpp as compared to phen is due to electron withdrawing effect of phenyl substituents in the former.

The cyclic voltammetric data of $[M(N\text{-}N)X_2]$ are given in Table 4. One of the representative voltammograms is given in Fig. 3. In general the complexes show diffuse, irreversible and successive two one-electron reductions and one quasi-reversible one-electron oxidation. The irreversibility of the reduction peaks was confirmed by the absence of the peak in the reversible scan or the large difference in potentials between two counter peaks. The general electron transfer series for the complexes $[M(N\text{-}N)X_2]$ can be represented as

$$[M(N\text{-}N)X_2]^+ \underset{-e^-}{\overset{+e^-}{\rightleftharpoons}} [M(N\text{-}N)X_2]^0 \xrightarrow{+e^-} [M(N\text{-}N)X_2]^- \xrightarrow{+e^-} [M(N\text{-}N)X_2]^{2-}$$

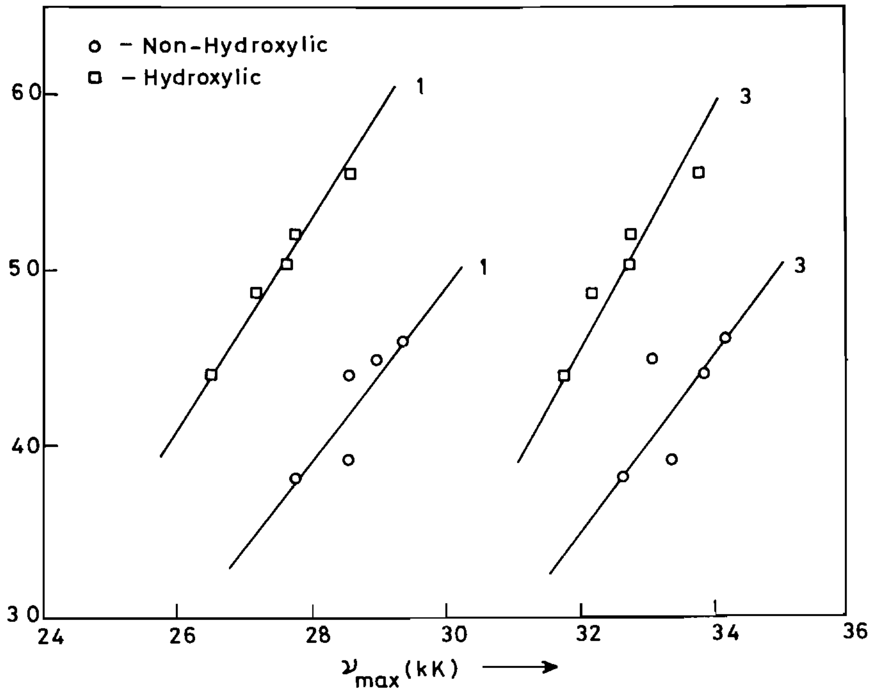

Fig. 2. Plot of E_T against ν_{max} for the charge transfer bands 1 and 3 of $[Pd(bipy)(N_3)_2]$.

TABLE 3. Electronic absorption spectral data of [M(N-N)X$_2$] complexes in DMF

Complex	Band maxima in kK			
	Band 1	Band 2	Band 3	Band 4
[Pd(bipy)Cl$_2$]	26.67(sh)^a	31.49 (13.47)^b	32.47 (12.88)	37.62 (8.53)
[Pd(biq)Cl$_2$]	28.04 (10.46)	29.53 (22.94) 30.79 (26.48)	32.34 (29.08)	36.87 (36.20)
[Pd(phen)Cl$_2$]	27.96 (1.93)	29.34 (2.03)	33.55 (1.28)	35.94 (28.68) 38.46(sh)
[Pd(dpp)Cl$_2$]	27.01 (9.70)	30.30(sh)	34.06 (56.80)	38.14 (38.70)
[Pt(bipy)Cl$_2$]	25.71 (3.63)	30.69 (9.93) 31.85 (8.59)	35.71 (21.11)	38.40(sh)
[Pt(biq)Cl$_2$]	26.18 (1.80)	29.53 (23.79) 30.75 (30.20)	31.89 (27.86)	37.29 (32.08)
[Pt(phen)Cl$_2$]	25.51 (3.55)	27.03 (2.89) 30.58 (5.15)	35.71 (20.47)	37.31(sh)
[Pt(dpp)Cl$_2$]	24.70 (3.29)	29.46 (6.35)	33.62 (16.62)	37.26 (14.54)
[Pd(bipy)(N$_3$)$_2$]	28.57(sh)	31.53 (23.94)	33.90 (25.51)	36.96 (26.58)
[Pd(biq)(N$_3$)$_2$]	27.03(sh)	29.59(sh) 30.69 (36.15)	32.26 (35.00)	37.15 (35.45)
[Pd(phen)(N$_3$)$_2$]	27.66 (7.75)	31.25(sh)	32.46(sh)	36.02 (44.08)
[Pd(dpp)(N$_3$)$_2$]	26.46 (6.50)	30.30(sh)	34.22 (41.76)	37.04(sh)
[Pt(bipy)(N$_3$)$_2$]	25.02 (4.19)	30.77 (8.14)	34.84 (19.45)	37.04(sh)
[Pt(biq)(N$_3$)$_2$]	26.67 (0.35)	29.53 (3.18) 30.68 (3.95)	31.75 (3.65)	37.26 (4.27)
[Pt(phen)(N$_3$)$_2$]	24.84 (5.89)	28.62 (6.80)	34.48(sh)	37.01 (34.14)
[Pt(dpp)(N$_3$)$_2$]	24.39(sh)	28.20 (11.70)	33.92 (37.69)	35.71(sh)

^{a}Shoulder. ^{b}Molar extinction coefficient in l mol^{-1} cm^{-1} × 10^{-3} are given in parentheses.

The potentials of the first reduction and oxidation of the [M(N-N)X$_2$] may be related to the nature of the orbitals involved in these redox processes. These orbitals are HOMO consisting predominately of the $d_{x^2-y^2}$ orbital and the LUMO consisting of the π^* orbital of α-diimine [18]. The higher positive value of the first oxidation potential of [Pd(bipy)Cl$_2$] and [Pd(biq)Cl$_2$] compared to the corresponding platinum

TABLE 4. Electrochemical data of $[M(N\text{-}N)X_2]$ complexes in CH_3CN[a]

Complex	Reduction			Oxidation	
	I	II	III	I′	II′
$[Pd(bipy)Cl_2]$	−0.40	−0.85		+0.90	
$[Pd(biq)Cl_2]$	−0.50	−1.15		+0.90	
$[Pd(phen)Cl_2]$	−0.75	−1.00		+0.80	
$[Pd(dpp)Cl_2]$	−0.38	−0.80		+0.80	
$[Pt(bipy)Cl_2]$	−0.40	−1.25		+0.75	
$[Pt(biq)Cl_2]$	−0.40	−1.20		+0.60	
$[Pt(phen)Cl_2]$	−0.70	−1.28		+0.85	+1.00
$[Pt(dpp)Cl_2]$	−0.35	−1.15		+0.80	
$[Pd(bipy)(N_3)_2]$	−0.50	−1.10		+0.75	
$[Pd(biq)(N_3)_2]$	−0.65	−1.05		+0.80	
$[Pd(phen)(N_3)_2]$	−0.50	−0.75		+0.80	
$[Pd(dpp)(N_3)_2]$	−0.30	−1.10		+0.70	+1.00
$[Pt(bipy)(N_3)_2]$	−0.42	−1.22		+0.75	
$[Pt(biq)(N_3)_2]$	−0.45	−1.10		+0.80	+1.15
$[Pt(phen)(N_3)_2]$	−0.68	−0.95	−1.15	+0.80	+1.20
$[Pt(dpp)(N_3)_2]$	−0.40	−1.15		+0.72	+1.05

[a] Potentials in volts vs. Ag/AgCl.

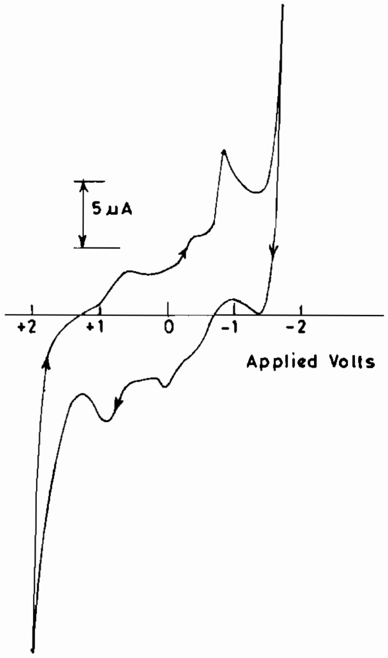

Fig. 3. Cyclic voltammogram of 3 mM of $[Pd(bipy)Cl_2]$ in 0.1 M $(C_4H_9)_4NClO_4$ in acetonitrile; scan rate 0.2 V s^{-1} at 6 mm outer diameter platinum electrode; potential in volts vs. Ag/AgCl.

complexes (see Table 4) can be explained in terms of the higher energy of $d_{x^2-y^2}$ in platinum than in palladium [19]. This behaviour is not observed in the corresponding azido complexes. The small negative reduction potential of $[M(dpp)(N_3)_2]$ as compared to $[M(phen)(N_3)_2]$ can be explained in terms of lowering of the energy of dpp compared to phen due to the electron withdrawing effect of phenyl groups in dpp. The large negative reduction potential of $[M(phen)Cl_2]$ as compared to other $[M(N\text{-}N)Cl_2]$ cannot be explained by the above model, but can be explained by the different extent of back bonding from d_π orbitals of the metal to π^* antibonding orbital of α-diimine.

The observed difference between the redox potentials and the energy of absorption band 1 can be explained in terms of the dependence of the redox potential of an irreversible electron transfer process on both the kinetic and thermodynamic parameters and the energy of absorption on only the thermodynamic parameter [20].

Acknowledgements

We thank the DST (Government of India) for financial support of this research. S.S. Kamath (SRF) is also thankful to CSIR, New Delhi, for financial assistance. We are grateful to Prof. G. Govil for allowing us to use the 500 MHz NMR facility at T.I.F.R., Bombay.

References

1 A. Vogler and H. Kunkely, *Angew. Chem., Int. Ed. Engl., 21* (1982) 209.
2 S. Shukla, S. S. Kamath and T. S. Srivastava, *J. Photochem. Photobiol., A: Chemistry, 44* (1988) 143.
3 B. S. Furniss, A. J. Hannaford, V. Rogers, P. W. G. Smith and A. R. Tachell, *Vogel's Textbook of Practical Organic Chemistry*, Longman, London, 1978, pp. 264–279.

4 F. A. Palocsay and J. V. Rund, *Inorg. Chem., 8* (1969) 524.

5 B. J. Malormiek, E. N. Joyes, Jr. and R. I. Kaplan, *Inorg. Synth., 13* (1971) 217.

6 V. Kumar, M. M. Rao and N. Ahmed, *Ind. J. Chem., 17* (1979) 305.

7 P. M. Gidney, R. D. Gillard and B. T. Heaton, *J. Chem. Soc., Dalton Trans.,* (1973) 132.

8 L. A. Rossiello, *Gazz. Chim. Ital., 97* (1968) 1177.

9 J. L. Burmeister and F. Basolo, *Inorg. Chem., 3* (1964) 1589.

10 W. J. Geary, *Coord. Chem. Rev., 7* (1971) 81.

11 K. Nakamoto, *Infrared and Raman Spectra of Inorganic and Coordination Compounds,* Wiley-Interscience, New York, 4th edn., 1986, pp. 231, 290–291.

12 J. E. Sarneski, L. E. Rickson and C. N. Reilley, *Inorg. Chem., 20* (1981) 2137.

13 L. Kumar, K. H. Puthraya and T. S. Srivastava, *Inorg. Chim. Acta, 86* (1984) 173.

14 K. H. Puthraya and T. S. Srivastava, *Polyhedron, 4* (1985) 1579.

15 Asahi Research Centre (ed.), *Handbook of Proton NMR Spectra and Data,* Academic Press, New York, 1985, Vol. 4, pp. 17, 239; Vol. 5, pp. 237, 356.

16 A. P. B. Lever, *Inorganic Electronic Spectroscopy,* Elsevier, Amsterdam, 2nd edn., 1984, pp. 203–376.

17 J. Burgess, *Spectrochim. Acta, Part A, 26* (1970) 1369.

18 M. Martin, M.-B. Krogh-Jespersen, M. Hsu, J. Tewksbury, M. Laurent, K. Vishwanath and H. Patterson, *Inorg. Chem., 22* (1983) 647.

19 W. L. Jolly, *Modern Inorganic Chemistry,* McGraw-Hill, New York, 1984, p. 409.

20 J. A. Davies, V. Uma and J. G. Mierzwiak, *J. Electroanal. Chem., 196,* (1985) 329.